COPY RIGHT

Dr. Bhargavi Peddireddy, Venkata Sai Chaitanya Kolliboyina,

Kamal Kumar Tiruveedula

USE THIS BARCODE TO ACCESS YOUR ONLINE PAPER

To Secure Your Paper As Per UGC Guidelines We Are Providing A Electronic Bar Code

Cyclone Intensity Estimation Using Pre- Trained Deep Learning Models

[1]Dr. Bhargavi Peddireddy
Associate Professor, Dept of Artificial Intelligence,
Vidya Jyothi Institute of Technology, Hyderabad, India
bhargavi.peddyreddy@gmail.com
[1*]Venkata Sai Chaitanya Kolliboyina
Dept of Artificial Intelligence,
Vidya Jyothi Institute of Technology, Hyderabad, India
kvschaitanya17@gmail.com
[2]Kamal Kumar Tiruveedula
Dept. of Artificial Intelligence,
Vidya Jyothi Institute of Technology, Hyderabad, India tiruvidulak@gmail.com

Abstract

Every year in India, One of the biggest hazards to property and human life is posed by tropical cyclones. They comprise a number of dangers, including as storm surge, flooding, extremely strong winds, tornadoes, and lightning, any of which can have a considerable negative impact on life and property. These risks interact with one another, significantly raising the possibility of fatalities and property damage. According to a study on extreme weather events, as many as 117 cyclones hit India in 50 years from 1970 to 2019, claiming over 40,000 lives. However, the mortality rate due to tropical cyclones has decreased significantly over the last ten years. Due to advancements in technology, detection of cyclones became much easier. Cyclones are categorized into various categories based on their intensity which is calculated by various methods and sources. Estimation of the intensity of cyclone helps them to categorize. Based on that the government and people can take precautionary measures to avoid the huge loss of life and property. India meteorological Department uses the Tropical Cyclone Intensity Scale to categorize the cyclones into 7 categories. For this project we are using the INSAT3D Infrared & Raw Cyclone Imagery (2012-2021 from the kaggle. The Raw Data has been sourced from the MOSDAC server. It consists of cyclone images, infrared images of cyclones. It consists of 140 images of cyclones from 2012-2021 that were happened around India. In this project we are trying to estimate the intensity of cyclones using the- state-of-the-art deep learning models as they are pre-trained

on the large datasets. We are using Four pre-trained deep learning models to compare the results of this approach.

Keywords: Tropical cyclones, Cyclone intensity estimation, MOSDAC, Indian Meteorological department,

Introduction

Tropical cyclones and their associated storm surges can affect a lot of locations worldwide. Despite enormous efforts, many people perish in storm attacks every year. Due to its potential influence on the economy and concerns over public safety, A significant field of research is precise intensity estimation of tropical cyclones (TC). To accurate anticipate TC intensity, a precise measurement of the current wind speed is required.

A tropical cyclone (TC), a type of storm system, is defined as large air masses moving in polar opposite directions—clockwise in the Southern Hemisphere and counter-clockwise in the Northern Hemisphere.Its centre, or "eye," is surrounded by intense thunder storms, low air pressure, and heavy rain. The eye wall, or the ring area surrounding the eye, is where the wind and rain are observed to be moving the fastest. The radius and eye diameter of the medium-sized TC are 300–600 km and 30–60 km, respectively. When humid air rises and releases heat by concentrating water vapour, TC is created over a sizable expanse of warm ocean water. A cyclone must have a number of environmental conditions in order to form, such as ocean waters that are at least 26.5°C from the surface to 50 m below the surface. However, the mechanisms behind how a tropical cyclone forms are still poorly understood. The minimum sea level pressure (MSLP) or surface maximum sustained wind speed (MSW), which is the average wind speed over one minute, are used to determine how intense a TC is. The MSW is calculated as the average wind speed for a period of 10 minutes everywhere in the world besides the United States. Tropical cyclones in the Atlantic and Eastern North Pacific are classified as Tropical Depressions if their winds are less than 34 kt, Tropical Storms if they are between 34 kt and 63 kt, and Hurricanes if they are over 64 kt. Different intensity thresholds and other subcategories are employed in other ocean basins, such as the Indian Ocean. An area of low pressure that forms over tropical or subtropical oceans is known as a tropical cyclone. With the exception of the South

Atlantic and the eastern South Pacific, which are located east of around 140º W longitude, these systems form throughout all tropical oceans. Tropical cyclones frequently originate in the following seven tropical storm basins:

1. The Atlantic Ocean

2. the Northeast Pacific basin

3. North Indian Basin

4. Southwest Indian Basin

5. The Indian/Australian subcontinent

6. Northwest Pacific Basin

7. Australian/Southwest Pacific Basin

Since TCs spend a large portion of their lives in the ocean, these measurements are uncommon for them. On the other hand, satellite photos can be used to remotely explain the dynamics, traits, and structure of TCs (Ritchie et al., 2003; Velden et al., 2006a). Since 1960, satellites have made it possible to observe the TCs. Today, satellite series offer nearly total coverage of the tropics, where conventional meteorological observations are uncommon. The primary technique for estimating TC intensity is based on satellite measurements. Two of the most widely used bands are infrared and visible, which offer details on the composition and location of atmospheric systems. The thermal infrared band (8 µm – 16 µm) receives light released from the tops of clouds and is constantly available. However, solar energy from the tops of the clouds is dispersed and reflected in the visible channels (0.35 µm to 0.7 µm). As a result, this information is not accessible at night. information regarding those pathways cannot supply the lower layers of the atmosphere's atmospheric systems because they are frequently obscured by clouds.

When direct measurements of environmental parameters like temperature and pressure are unavailable, the recognition of typical circular and curved patterns using remotely sensed data is one potential technique to determine the origin and evolution of tropical cyclones. Dvorak developed the first thorough approach for analysing patterns to gauge the strength of tropical storms from satellite photography (Dvorak, 1972, 1975, 1984). Despite being subjective, many TC forecasting stations across the world continue to use the Dvorak technique (DT) as their primary intensity estimation and forecasting approach (Velden et al., 2006a). For ocean basins without aircraft reconnaissance, tropical

International Journal for Innovative Engineering and Management Research
A Peer Reviewed Open Access International Journal

www.ijiemr.org

cyclone forecasters can only estimate TC intensity using satellite-based methods. A specialist uses the method by adhering to a set of experimentally established guidelines to measure cloud properties in satellite photos. These techniques are used by the expert to locate the final intensity estimate in a lookup table. But the DT is arbitrary, time-consuming, and user-experience- dependent. The objective Dvorak technique (ODT), a development of the original DT that utilised computer- based analysis to assess intensity (Velden et al., 1998). The advanced objective Dvorak technique (AODT) was created to get over some of the drawbacks of the ODT, like the need to manually choose the storm centre or the inability to work with weak storms. The advanced Dvorak technique (ADT) is the most recent iteration of ODT (Olander and Velden, 2007). The ODT and AODT, on the other hand, concentrated on mimicking the subjective technique, whilst the ADT focuses on expanding the method beyond its initial application and limitations. The wind vector field can also be estimated using remotely sensed imagery. Automated methods for estimating the intensity based on wind speed could be based on creating a wind vector field from a series of

photographs. The typical methods for creating a vector field out of a collection of images include cross correlations (González and Woods, 2002) and optical flow (Horn and Schunck, 1981). These methods offer two ways to identify and quantify object movement by comparing pixels across image sequences. However, slight and smooth differences in the pictures are necessary for the accurate identification and assessment of object movements. But it's uncommon to find photos with such great temporal resolution.

For ocean basins without aircraft reconnaissance, the only method available to forecasters for determining the severity of Tropical Cyclones (TC) is the satellite-based approach. The most used method for calculating TC intensity from visible and infrared satellite pictures is the Dvorak technique (DT). Depending on cloud patterns in satellite images, DT uses a T-number scale (the storm category number based on current intensity), as given in Table 1, to predict TC intensity. However, the original DT was arbitrary, labor-intensive, and predicated on the expertise of an expert. Despite this, many TC forecasting centres across the world continue to utilise the DT as their primary intensity

International Journal for Innovative Engineering and Management Research
A Peer Reviewed Open Access International Journal
www.ijiemr.org

estimation tool (Knaff et al., 2010; Velden et al., 2006a; Velden et al., 1998). Traditionally the cyclone intensity estimation is calculated using statistical methods in which a renowned technique called Dvorak Technique is used. Later other advanced techniques are proposed based on the Dvorak Technique. Even with these advanced methods it becomes a tedious task by following various steps in the Dvorak and advanced Dvorak techniques which results in delay in forecasting the information.

Figure 1.1 shows how to calculate the T-number using DT (Dvorak, 1984), which is a collection of empirical rules. This process contains ten phases and a number of substeps, as shown in the demonstration. It included spatial patterns in the visible and infrared spectra brightness temperatures (BT) of the clouds.

CI number 1.0	MWS (kts)25	MSLP (hPa)

1.5	25	----
2.0	30	1009
2.5	35	1005
3.0	45	1000
3.5	55	994
4.0	65	987
4.5	77	979
5.0	90	970
5.5	102	960
6.0	115	948
6.5	127	935
7.0	140	921
7.5	155	906
8.0	170	890

An expert uses the method to subjectively measure a number of cloud properties in the image. The experts locate the atmospheric disturbance's centre, then examine its location in relation to the pattern's cold clouds to assess the strength of the TC. By examining the cloud pattern of the storms, the strength was calculated in two different ways. Step 2 begins with estimating intensity by assessing the cloud characteristics that were associated with storm intensity. When the cloud features in the analysed cloud pattern matched those in the cloud types mentioned in steps 2A through 2E as depicted in Figure 1.2, this step is finished. For instance, pattern T number (PT) 1.5 would be transmitted to the TC if the band of the pre-curve storm could be found. If the intensity estimate supplied by step 2 came within the defined boundaries, the measurement

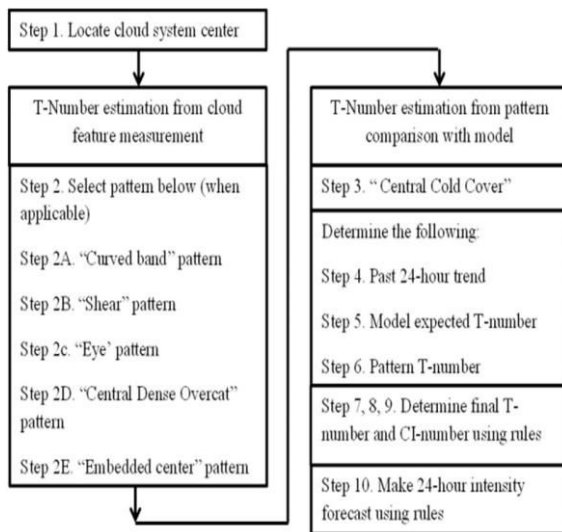from that step would be utilised as the final intensity.

Figure 1.1. DT intensity estimation method. (Dvorak, 2004)

Later on, the third phase is discussed. Steps 4 through 6 are used to determine the second intensity estimate. When observations of the storm features were not available, steps 4 and 5 created an intensity estimate known as the model expected T-number (MET). They also specified the parameters that had to be met by the measured estimations. A storm's MET is calculated by comparing its most recent image with its previous image from the previous day and determining whether or not the storm has continued along its previous course of development. The estimated intensity could then be calculated by extrapolating along the model's intensity change curve, which was the one that best fit the storm's historical evolution. To get this intensity estimate, for instance, the expert would just need to identify the pattern that best describes the storm by studying it over a 24-hour period to achieve this intensity estimate for the "Curved-Band Pattern" type.

The intensity estimate from step 5 is modified in step 6. This estimate of intensity would then be used when storm intensity-related cloud features are observable but not distinct enough for measurement. This compares the cloud pattern of the storm to patterns in the model that matched the stage of development indicated in step 5. The intensity estimate is then revised up or down when the cloud pattern under examination appears to be obviously stronger or weaker than was anticipated based on its earlier growth rate. Steps 7 through 9 involve testing the intensity estimate derived from the cloud features in accordance with the technique's principles (described in section 3.4.1) to see if it fits within predetermined bounds or if it needs to be changed.
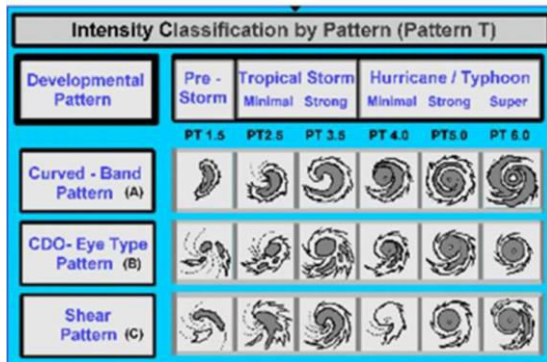
Figure 1.2: advancements in the sorts of cloud patterns employed in intensity analysis. Typical 24-hour alterations are shifts in the pattern from left to right. (Tropical, 2013)

Step 3, which was previously omitted, is applied when the cloud pattern indicated a centre cloud cover (CCC). A CCC pattern is when the storm centre or comma head, which has the appearance of a comma, is obscured by a mass of clouds that is more or less spherical and conceals the expected pattern progression rings (Dvorak, 1984). The storm's development stops when this pattern type emerges (or soon will). The final step of the method provided instructions for forecasting 24-hour intensity.

This article's organisation is as follows. Section II describes about the dataset collection and data set preperation. Section III consists of the methodology and related concepts. Section IV consists of describes the performance evaluation of the proposed methodology. Section V consists of conclusions of this article.

About Dataset

The ISRO launched the INSAT constellation of geostationary satellites, also referred to as the Indian National Satellite System, to serve India's telecommunications, broadcasting, meteorology, and rescue and recovery needs. In 1983, INSAT launched the largest home communication network in the Asia Pacific region. Hassan and Bhopal's Master Control Facilities keep an eye on and manage the satellite. A multipurpose geosynchronous spacecraft with a focus on meteorology is INSAT-3D. (imager and sounder). The primary goals of this mission are to develop an operational system for weather, environmental, and storm warnings to save people and property. Oceanic observations are being tracked by INSAT3D, which also offers data transmission options. Through two S-band transponders, it offers Broadcast Satellite Services (BSS). Visible, shortwave infrared, middle infrared, water vapour, and two bands in the thermal infrared areas are among the six wavelength bands that the multi-spectral imager (optical radiometer) on board the INSAT-3D spacecraft

may use to create photographs of the globe. The surveillance of mesoscale phenomena and powerful local storms is now possible thanks to the enhanced visible band resolution of 1 km.

Dataset description

Image Dataset containing all INSAT3D captured INFRARED and RAW Cyclone Imagery over the Indian Ocean from 2012 to 2021 along with each Cyclone Image intensity in KNOTS. The Raw Data has been sourced from the MOSDAC server and have labelled each Image by locating the timestamp with its respective coordinate in the intensity-time graph of each cyclone directory. Originally curated by Sshubam Verma. In entire dataset, only Infrared cyclone images were taken and a csv file is made with the images and the intensity values. It was used for loading the data.

Data Preperation

Data from the server consists of 3 types of images viz. infrared, raw, and reference images. All the Infrared images are stored in a single folder and the data is loaded using keras image data generator and flow from

dataframe methods with various parameters. Flow from dataframe method takes the dataframe and path to the directory and generate batches. The generated batches contain augmented, normalised data. Each image is resized to 224,224,3 and normalised.

Methodology

Instead of following the statistical approach for calculating the intensity of cyclone, we are using the state-of-the-art deep learning models on the infrared satellite images of INSAT 3D which was launched by ISRO for weather observation. These State-of-the-art deep learning models include ResNet50,InceptionV3, Densenet201, InceptionResnetV2. These models were chosen because of less number of parameters to train which results in less computation power and less training time.
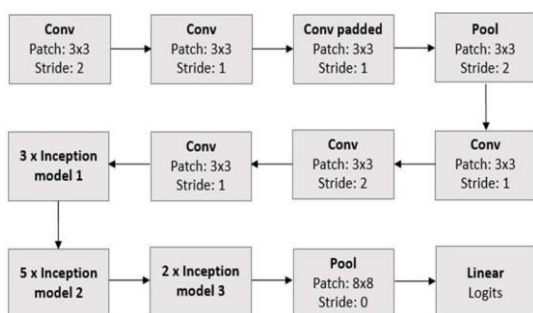
Inception V3

A deep learning model for categorising images that is focused on convolutional neural networks is called Inception V3. The core model Inception V1, that was released in 2014 as GoogLeNet, was upgraded with the Inception V3. As the

International Journal for Innovative Engineering and Management Research
A Peer Reviewed Open Access International Journal
www.ijiemr.org

name suggests, a Google team designed it (Opengenius, 2022). Simply said, the inception V3 model is the inception V1 model with improvements and optimizations. The Inception V3 model optimised the network using a number of techniques to increase model adaptability.

- It is more efficient.
- It has a larger network than the Inception V1 and V2 models, yet its speed is not affected.
- It is less computationally expensive.
- It uses auxiliary Classifiers as regularizers.

The 42 layers and lower error rate of the Inception v3 model, which was introduced in 2015, distinguish it from its forerunners. Let's examine the several optimizations that make the Inception V3 model better. The inception V3 model has a total of 42

layers, which is a little increase over the inception V1 and V2 models. However,

this model's effectiveness is quite impressive. Figure 3.1 shows the inception V3 architecture.

ResNet50

Training more complex neural networks is more challenging. When deeper networks can start to converge, a degradation issue arises: as network depth rises, accuracy gets saturated (which is not entirely unexpected) and rapidly degrades. Surprisingly, such degradation is not the result of overfitting because, as stated in and strongly supported by our testing, adding more layers to a sufficiently deep model increases training error. The decline in training accuracy shows that not all systems are equally amenable to optimization (Kahe, 2015). One MaxPool layer, one Average Pool layer, and 48 Convolution layers make up the ResNet50 model version. It has a floating point operation capacity of 3.8 x 109. It is a popular ResNet model. In the 2012 LSVRC2012 classification competition, AlexNet took first place. Ever since, ResNet has been the most exciting development in the fields of deep learning and computer vision.

Figure 3.1: Basic architecture of Inception V3

Numerous computer vision applications are built on the conventional neural network known as ResNet, or Residual Networks. This model triumphed in the 2015 ImageNet competition. It was able to train ultra-deep neural networks, which implies that a network may contain hundreds or thousands of layers and yet function properly, thanks to the foundation that ResNets offered. Skip connection was first introduced by ResNet. There are around 23 million trainable parameters in the ResNet-50. ResNets were first used for image recognition tasks, but the architecture can also be used to boost accuracy for non-computer vision activities, according to the study. As a result of the effectively reduced training error, ResNet minimizes the top-1 error by 3.5%. The following component is a part of the Resnet50 architecture:
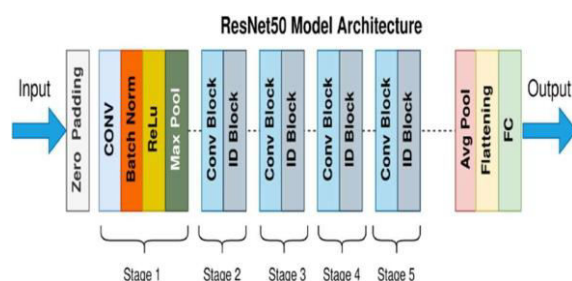
- One layer is produced using convolution with a kernel size of 7 *

7 and 64 different kernels, each with a stride size of 2.

- • Max pooling with a 2 stride size is then followed by

- A 1 * 1,64 kernel appears in the subsequent convolution, which is followed by a 3 * 3,64 kernel and a 1 * 1,256 kernel. We have nine levels in this phase thanks to the repetition of these three layers a total of three times.

- Then, a kernel of 1 * 1,128 is visible, then one of 3 * 3,128, and lastly one of 1 * 1,512. We

completed this phase four times, adding up to a total of 12 layers.

- There are then two further kernels of 3 * 3,256 and 1 * 1,1024, which are repeated six times for a total of 18 layers. The last kernel is 1 * 1,256.

- A 1*15,512 kernel was next, followed by two more kernels of 3*3,512 and 1*1,2048. This process was done three times for a total of nine layers.

- Next, we run an average pool, and last, we produce a fully linked layer with 1000 nodes and a softmax function, resulting in one layer (Opengenius, 2021)
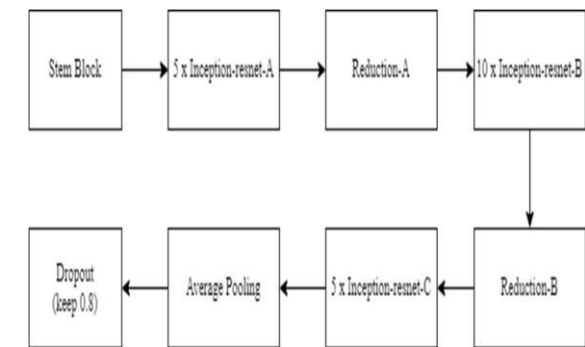
Figure 3.2: ResNet50 architecture

InceptionResNet V2

Over a million images from the ImageNet collection served as the training data for the Inception-ResNet-v2 convolutional neural network. The 164-layer network can classify images into 1000 different object categories, including the mouse, keyboard, pencil, and numerous animals. The network has therefore acquired in-depth feature representations for a wide range of images. The network outputs a list of estimated class probabilities after receiving a 299 by 299 image as input. It is made by fusing the Residual connection and the Inception structure. In the Inception-Resnet block, residual connections are combined with convolutional filters of various sizes. Relative connections are added, which not only addresses the degradation problem brought on by deep structures but also speeds up training. The fundamental structure of Inception-Resnet V2 is depicted in Figure 3.2.

DenseNet201

The network can be narrower, more streamlined, and have fewer channels since each layer obtains feature maps from all layers that passed before it. The extra number of channels for each layer is the growth rate k.

The "vanishing gradient" problem, meanwhile, only becomes apparent as the CNN gets deeper or has more layers. This means that when the separation between the input and output layers grows, some knowledge may "vanish" or "get lost," which reduces the network's capacity to learn effectively. By altering the standard CNN architecture and streamlining the connectivity between layers, DenseNets

alleviate this issue.

Figure 3.3: inception-Resnet V2 architecture

A convolutional neural network with 201 layers is called DenseNet-201. The ImageNet database contains a pretrained version of the network that has been trained on more than a million photos. The pretrained network can categorise photos into 1000 different object categories, including several animals, a keyboard, a mouse, and a pencil. The network has therefore acquired rich visual features for a variety of images. The

network accepts images with a resolution of 224 by 224. In a DenseNet, each layer broadcasts its own feature-maps to all layers that came after it and receives additional input from all layers that came before it. You combine two things together. The tiers below it provide "collective knowledge" to the layers above them. The growth rate k is the additional number of channels required for each layer.

When the size of feature maps varies, it is not possible to use the concatenation method. However, downsampling of layers, which minimises the size of feature-maps through dimensionality reduction to enable faster calculation speeds, is a crucial component of CNNs. This is made possible by the division of DenseNets into Dense Blocks, where the size of the feature maps inside a block is kept constant but the number of filters between them changes. Transition Layers are the layers in between the blocks that cut the number of channels in half compared to the number of channels currently in use. With every pre-trained model as base model, we added several layers to it before the output layer which includes gloabal average pooling2d, batchNormalisation, flatten and dropout.

At output layer of each pre-trained model, Linear activation function is used as the target value that we are trying to predict is a continuous value.
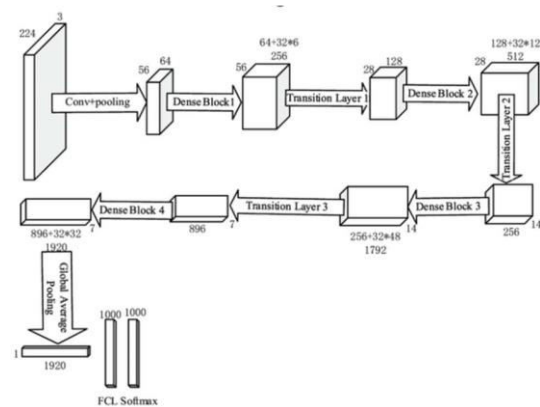

Figure 3.4: Densenet201 architecture

Performance Results

Every pre-trained model is trained for 50 epochs and their respective best model is saved using callbacks from keras library and later used for evaluating on validation and test data. We have trained every model on NVIDIA GeForce RTX 3050Ti GPU

Metrics: Mean Absolute Error (MAE) and a little about this is explained below.

One of the various measures used to summarise and assess a machine learning model's quality is MAE. As illustrated in the example below, the term "error" here refers to deducting the actual value from the anticipated value.

$Prediction\ Erro = Actual\ Value - Predicted\ Value$ (1)

Each record's prediction error is calculated, and then all errors are made positive. This is done by doing the following calculation on the Absolute value for each error:

$Absolute\ Error \rightarrow |Prediction\ Error|$ (2)

The mean for all reported absolute errors is then calculated (Average sum of all absolute errors).

$$MAE = \frac{\sum_{i=1}^{n} |y_i - x_i|}{n} \qquad (3)$$

Here, n represents the number of observations, y_i is the predicted value, x_i is the actual value, and n is the value

Resnet

First model is built with Resnet50 as a base model and the trainable layers are set to freeze so that model weights doesn't change with training. Final model consists of 270,849 trainable parameters and 23,587,968 non-trainable parameters. It results in 13.512 as Mean Absolute Error (MAE) on validation data and 45.324 on test data. Below graph shows the training and validation losses graphs of the Resnet50 model.
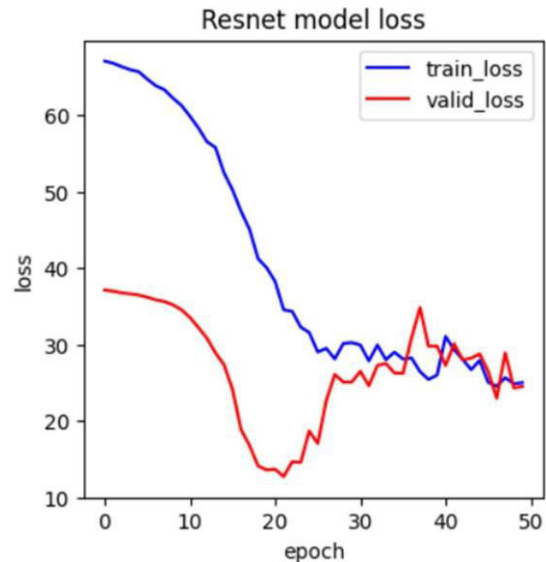

Figure 4.1: Training and validation loss of ResNet50

Resnet model's predictions on the test data are displayed in the picture below.
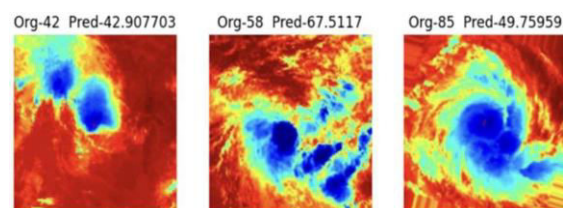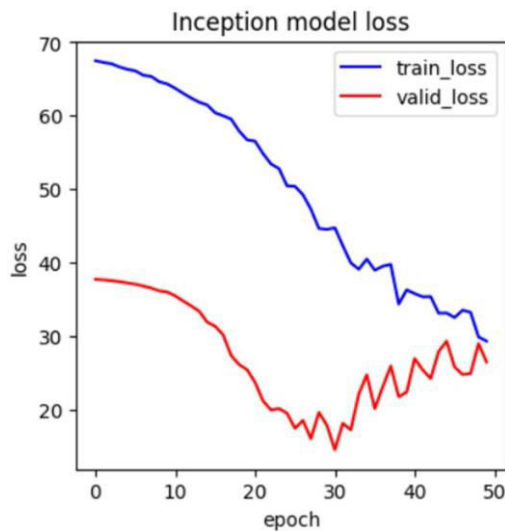

Figure 4.2: Predictions of ResNet50 on the test data

InceptionV3

International Journal for Innovative Engineering and Management Research
A Peer Reviewed Open Access International Journal
www.ijiemr.org

Second model is built with InceptionV3 as a base model and the trainable layers are set to freeze so that model weights doesn't change with training. Final model consists of 270,849 trainable parameters and 21,803,040 non-trainable parameters. It results in **18.030** as Mean Absolute Error (MAE) on validation data and **42.889** on test data.Below graph shows the training and validation losses graphs of the Inceptionv3 model.

Figure 4.3: Training and validation loss of

InceptionV3 model

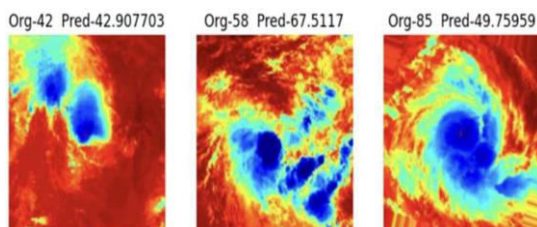InceptionV3 model's predictions on the test data are displayed in the picture below.

Figure 4.4 : Predictions of InceptionV3 on the test data

InseptionResnet V2

Fourth model is built with InceptionResnetV2 as a base model and the trainable layers are set to freeze so that model weights doesn't change with training. Final model consists of 205,313 trainable parameters and 54,336,992 non-trainable parameters. It results in 14.256 as Mean Absolute Error (MAE) on validation data and 33.849 on test data. Below graph shows the training and validation losses graphs of the Densenet201 model.
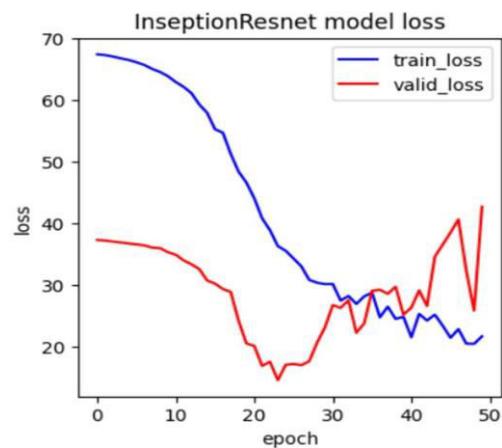

Figure 4.5: Training and validation loss of InseptionResnetV2 model

InceptionReesnetV2 model's predictions on the test data are displayed in the picture below.
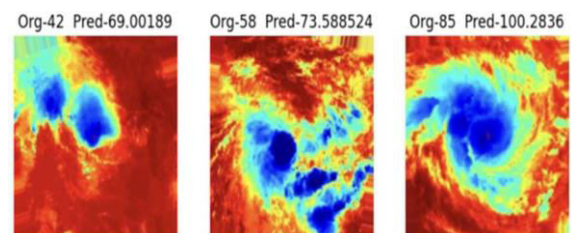

Figure 4.6 : Predictions of InceptionResnet V2 on the test data

Densenet201

Third model is built with InceptionV3 as a base model and the trainable layers are set to freeze so that model weights doesn't change with training. Final model consists of 254,465 trainable parameters and 18,322,240 non-trainable parameters. It results in **13.334** as Mean Absolute Error (MAE) on validation data and **42.523** on test data. Below graph shows the training and validation losses graphs of the Densenet201 model.
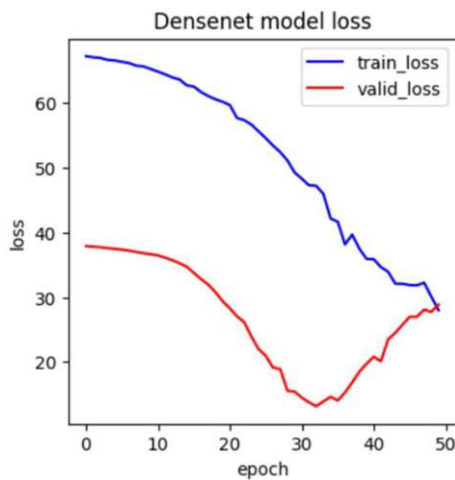

Figure 4.7: Training and validation loss of Densenet201 model

Densenet model's predictions on the test data are displayed in the picture below
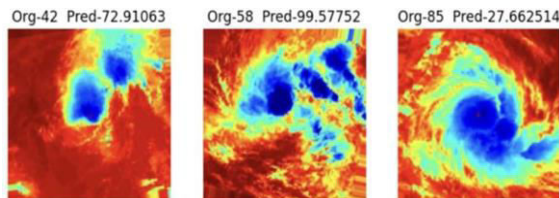

Figure 4.8 : Predictions of Densenet 201 on the test data

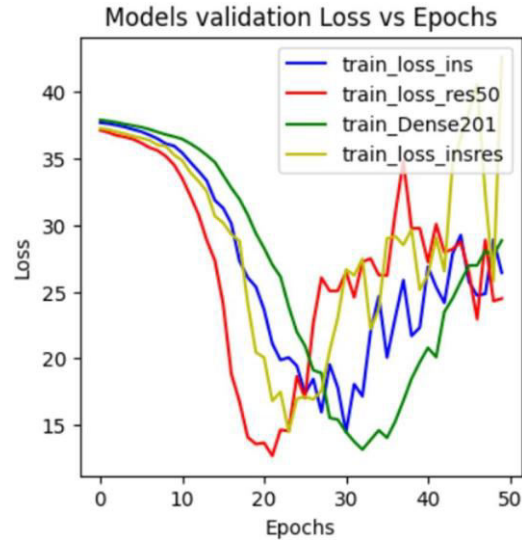The below graph shows the combined graph of all models loss on the validation data

Figure 4.9 : Models validation losses on the validation data

Model Name	Training Loss	Validation Loss	Test Loss
Resnet50	40.839	13.512	45.324
InceptionV3	42.899	18.030	37.899
Densenet 201	41.250	13.334	42.533
InceptionResnetV2	38.038	14.256	33.849

Table 4.1 : Table showing the evaluation metrics of all the pre- trained models used

Conclusion and Further Discussions

Traditionally the cyclone intensity estimation is calculated using statistical methods in which a renowned technique called Dvorak Technique is used. But the direct approach using the infrared

satellite images is a quick method when compared to the traditional statistical method. Using the pre-trained deep learning models makes it much faster and easier because of the training done on the previous data. To test this hypothesis we have used four pre-trained models on the INSAT-3D infrared satellite images which consists of various cyclones data over the past years. On training these models for 50 epochs each on NVIDIA GeForce RTX 3050Ti, Densenet 201 performed better on the validation data where Inseption ResnetV2 performed better on the Test data. This indicates that this direct approach could be used to perform the cyclone intensity estimation. These four models are considered based on their top 1% accuracy and the computation power, size of the model.

Few improvements can be made to improve the predictions. The performance can be improved by training on the more data and setting a few layers to freeze so that certain layer weights are modified with training, and using high computational power for faster evaluations and betterment of architecture.

References

1 Lin, Y. L. (2007). *Mesoscale dynamics*: Cambridge University Press.

2 Olander, T. L., & Velden, C. S. (2004). The advanced objective Dvorak technique (AODT) – continuing the journey. Paper presented at the 26th Conference on Hurricanes and Tropical Meteorology, Miami, FL.

3 Olander, T. L., & Velden, C. S. (2007). The advanced Dvorak technique: Continued development of an objective scheme to estimate tropical cyclone intensity using geostationary infrared satellite imagery.

4 Olander, T. L., & Velden, C. S. (2008). ADT – advanced Dvorak technique users' guide (McIDAS7.23). Accessible at: http://cimss.ssec.wisc.edu/tropic2/misc/adt/inf o.html.

5 Olander, T. L., & Velden, C. S. (2009). Update on the UW-CIMSS advanced Dvorak technique (ADT). Paper presented at the the Metrological Satellite and Tropical Cyclone Conference, Pearl Harbor, HI.

6 Olander, T. L., & Velden, C. S. (2012). Current status of the UW-CIMSS advanced Dvorak technique (ADT). Paper presented at the 30th AMS Conference On Hurricanes and Tropical Meteorology, Ponte Vedra Beach, FL.

7 Piñeros, M. F., Ritchie, E. A., & Tyo, J. S. (2008). Objective measures of tropical cyclone structure and intensity change from remotely sensed infrared image data. Geoscience and Remote Sensing, IEEE Transactions on, 46(11), 3574-

3580.

8 Velden, C., Harper, B., Wells, F., Beven, J. L., Zehr, R., Olander, T., . . . McCrone, P. (2006a). The Dvorak tropical cyclone intensity estimation technique: A satellite-based method that has endured for over 30 years. Bulletin of the American Meteorological Society, 87(9), 1195-1210.

9 Velden, C., Herndon, D. C., Kossin, J., Hawkins, J., & DeMaria, M. (2006b). Consensus estimates of tropical cyclone intensity using integrated multispectral (IR and MW) satellite observations. Paper presented at the 27th Conference on Hurricanes and Tropical Meteorology, Monterey, CA.

10 Velden, C., Olander, T. L., & Zehr, R. M. (1998). Development of an objective scheme to estimate tropical cyclone intensity from digital geostationary satellite infrared imagery. Weather and Forecasting, 13(1), 172-186.

11 Wimmers, A. J., & Velden, C. S. (2010). Objectively determining the rotational center of tropical cyclones in passive microwave satellite imagery. Journal of Applied Meteorology and Climatology, 49(9), 2013- 2034.

12 https://iq.opengenus.org/architecture-of- densenet121/

13 Sheu, S.-M., & Chou, J.-H. (2004). Automatic recognition of two-dimensional vortices by digital image processing. Journal of Flow Visualization & Image Processing, 11(4), 269-279.

14 González, R. C., & Woods, R. E. (2002). Digital image processing: Prentice Hall.

15 Han, J., & Kamber, M. (2006). Data mining : Concepts and techniques (2nd ed.). Amsterdam ; Boston; San Francisco: Elsevier ; Morgan Kaufmann.

16 Herndon, D. C., & Velden, C. S. (2008). CIMSS TC intensity satellite consensus (SATCON) Paper presented at the Interdepartmental Hurricane Conference, Charleston, SC.

17 Horn, B. K. P., & Schunck, B. G. (1981). Determining optical flow. Artificial Intelligence, 17(1– 3), 185-203

18 Cangialosi, J. P., 2019: National Hurricane Center forecast verification report: 2018 hurricane season. National Hurricane Center, 73 pp., www.nhc.noaa.gov/verifification/pdf s/Verififi cation_2018.pdf.

19 Y. Quilfen, and B. Chapron, 2020: Extensive high-resolution Synthetic Aperture Radar (SAR) data analysis of tropical cyclones: Comparisons with SFMR flflights and best track. Mon. Wea. Rev., 148, 4545–4563, https://doi.org/10.1175/MWR-D-20-0005.1.

20 Sharma, N., M. M. Ali, J. A. Knaff, and P. Chand, 2013: A soft computing cyclone intensity prediction scheme for the western North Pacifific Ocean. Atmos. Sci. Lett., 14, 187–192, https:// doi.org/10.1002/asl2.438.

21 Shimada, U., H. Owada, M.

Yamaguchi, T. Iriguchi, M. Sawada, K. Aonashi, and K. D. Musgrave, 2018: Further improvements to the Statistical Hurricane Intensity Prediction Scheme using tropical cyclone rainfall and structural features. Wea. Forecasting, 33, 1587–1603, https://doi.org/10.1175/ WAF-D- 18-0021.1.

22 http://satellite.imd.gov.in/archive/

23 Sshubam Verma. (2022). <i>INSAT3D Infrared & Raw Cyclone Imagery (2012- 2021)</i> [Data set]. Kaggle. https://doi.org/10.34740/KAGGLE/D SV/3868 589

24 https://mosdac.gov.in/cyclone-genesis/archive/